DMD Fast Forward. Published on January 24, 2006 as doi:10.1124/dmd.105.008094
This article has not been copyedited and formatted. The final version may differ from this version.

DMD #8094

IN VITRO METABOLIC ACTIVATION OF THIABENDAZOLE VIA 5-HYDROXYTHIABENDAZOLE: IDENTIFICATION OF A GLUTATHIONE CONJUGATE OF 5-HYDROXYTHIABENDAZOLE

DEEPAK DALVIE, EVAN SMITH, ALAN DEESE and STEPHEN BOWLIN[1]

Pharmacokinetics, Dynamics and Metabolism (D.D., E.S and S.B.) and Analytical Research and Development (A.D.), Pfizer Global Research and Development, San Diego CA 92121.

DMD #8094

Running Title: Metabolic Activation of Thiabendazole *in vitro*

Corresponding Author:

Deepak Dalvie, Ph. D.

Pharmacokinetics, Dynamics and Metabolism Department,

Pfizer Global Research and Development,

Science Center Drive, San Diego,

CA 92121.

E-mail: deepak.dalvie@pfizer.com,

Phone: (858) 622-8016.

[1]Current Address: Arena Pharmaceuticals, San Diego CA

Text pages: 37

Tables: 1

Figures: 9

Schemes: 2

References: 38

Words in Abstract: 251

Words in Introduction: 561

Words in Discussion: 1063

Abstract

Thiabendazole (TBZ) is a broad-spectrum antihelmintic used for treatment of parasitic infections in animals and humans and as an agricultural fungicide for post-harvest treatment of fruits and vegetables. It is teratogenic and nephrotoxic in mice, and cases of hepatotoxicity have been observed in humans. Recent reports have demonstrated a correlation between 5-hydroxythiabendazole (5-OHTBZ) formation, a major metabolite of TBZ, and covalent binding of [14C]TBZ to hepatocytes, suggesting another pathway of activation of TBZ. Current in vitro studies were undertaken to probe the bioactivation of TBZ via 5-OHTBZ by P450 and peroxidases and identify the reactive species by trapping with reduced glutathione (GSH). Microsomal incubation of TBZ or 5-OHTBZ supplemented with NADPH and GSH afforded a GSH adduct of 5-OHTBZ and was consistent with a bioactivation pathway that involved a P450-catalyzed two-electron oxidation of 5-OHTBZ to a quinone imine. The same adduct was detected in GSH fortified incubations of 5-OHTBZ with peroxidases. The identity of the GSH conjugate suggested that the same reactive intermediate was formed by both these enzyme systems. Characterization of the conjugate by mass spectrometry and NMR revealed the addition of GSH at the 4-position of 5-OHTBZ. In addition, formation of a dimer of 5-OHTBZ was discernible in peroxidase-mediated incubations. These results were consistent with a one-electron oxidation of 5-OHTBZ to a radical species that could undergo disproportionation or an additional one-electron oxidation to form a quinone imine. Overall, these studies suggest that 5-OHTBZ can also play a role in TBZ-induced toxicity via its bioactivation by P450 and peroxidases.

Introduction

Thiabendazole (TBZ) (Fig. 1) is a broad-spectrum antihelmintic used for treatment of parasitic infections in animals and humans and an agricultural fungicide for post-harvest treatment of fruits and vegetables (Groten et al., 2000; Walton et al., 1999). It is recognized as a potent nephrotoxin which causes tubular necrosis leading to severe kidney damage, and a teratogen which results in impairment of mouse limb development and selective toxicity to the embryo Tada et al., 1992; Fujitani et al., 1999; Ogata et al., 1984; Mizutani et al., 1990). Irreversible binding of TBZ-related radioactivity to macromolecules and tissue protein in the mouse embryo has also been observed following oral dosing of [^{14}C]TBZ to pregnant mice (Yoneyama and Ichikawa, 1986). In humans, several isolated cases of hepatotoxicity such as intrahepatic cholestasis or micronodular cirrhosis have also been reported following TBZ administration (Manivel et al., 1987; Bion et al., 1995). It is currently believed that TBZ-induced nephrotoxicity is a result of P450-dependent oxidative cleavage of the thiazole moiety in TBZ to a proximate toxicant, thioformamide (Fig. 1) (Mizutani et al., 1994). However, mechanisms responsible for TBZ-induced hepatotoxicity in humans and teratogenicity in preclinical species are not clear.

TBZ is extensively metabolized in animals and humans (Tocco et al., 1966). The primary route of metabolism is the CYP1A2-catalyzed formation of 5-hydroxythiabendazole (5-OHTBZ), which is further converted to a glucuronide and a sulfate conjugate and is eliminated in the urine and bile (Coulet et al., 1998a; Rey-Grobellet et al., 1996; Coulet et al., 1998b; Wilson et al., 1973). Other metabolites such as 4-hydroxythiabendazole, 2-acetylbenzimidazole, N-methylthiabendazole and benzimidazole, have also been detected (Fujitani et al., 1991). Recent studies by Coulet and coworkers (Coulet et al., 2000) have shown good correlation in the covalent binding of the radiolabel to proteins and the formation of 5-OHTBZ in incubations of [^{14}C]TBZ with cultured human and rabbit hepatocytes. These studies have also shown that

treatment of CYP1A2-expressing liver cells with isolated [^{14}C]5-OHTBZ leads to significant covalent binding of the radiolabel (Coulet et al., 2000). Furthermore, 5-OHTBZ has been described to possess the same teratogenic potential as the parent drug, TBZ, as demonstrated in a limb bud culture system (Tsuchiya et al., 1987). A possible link between 5-OHTBZ and hepatic injury has also been established based on the relationship between systemic peak concentrations of 5-OHTBZ and the onset of TBZ toxicity (Coulet et al., 1998b). All the above reports suggest that TBZ-induced toxicity can also be exerted via bioactivation of its major metabolite, 5-OHTBZ.

Although several mechanisms for the metabolic activation of 5-OHTBZ and its adduct formation have been proposed, the chemical structure of the reactive species has not been identified (Coulet et al., 2000). Structural similarities between the 5-hydroxybenzimidazole portion of TBZ and *p*-amino substituted phenolic compounds such as acetaminophen (Fig. 1) suggests that 5-OHTBZ can undergo metabolic activation to quinone imine like species via oxidation by enzyme systems such as P450 or peroxidases such as, prostaglandin H synthase (PGS). *para*-Amino substituted phenols are known to undergo bioactivation to electrophilic quinone imines by these oxidative enzyme systems and covalently bind to cellular thiols or be scavenged by reduced GSH (Monks and Jones 2002; Potter and Hinson 1987a; Moldéus et al., 1982). The objective of the current study was to examine the ability of 5-OHTBZ to undergo oxidative bioactivation by these enzyme systems and structurally characterize the resulting reactive species by trapping with glutathione.

Materials and Methods

Materials. Thiabendazole, horseradish peroxidase (HRP; type VI-A, 1000 units/mg of protein), reduced glutathione (GSH), NADPH, arachidonic acid (AA) and hydrogen peroxide (30%) were obtained from Sigma/Aldrich (St. Louis, MO). Ram seminal vesicle microsomes (protein concentration 5 mg/mL) were purchased from Oxford Biomedical Research (Oxford, MI). Isopropylester of glutathione (GSH-IP) was obtained from Bachem (Torrance, CA). Human liver microsomes were prepared from human livers (International Institute for the Advancement of Medicine, Jessup, PA) using standard protocols and were characterized using P450-specific marker substrate activities. Aliquots from the individual preparations from 56 individual human livers were pooled on the basis of equivalent protein concentrations to yield a representative microsomal pool with a protein concentration of 20.4 mg/mL (determined using the Bicinchoninic Acid Assay; Pierce, Rockford, IL). Individual recombinant CYP1A2 co-expressed with NADPH-P450 oxidoreductase in baculovirus-infected insect cells were obtained from Panvera Corp. (Madison, WI). The protein concentration of the recombinant enzyme was 10.4 mg/mL and P450 content was 1.1 nmol/mL. Mouse liver and β-napthoflavone-treated rat liver microsomes (protein concentration, 20 mg/mL) were obtained from Xenotech LLC (Kansas City, KS). Other chemicals and reagents were of the highest quality available.

Microsomal Incubations of TBZ. The microsomal metabolism of TBZ was studied using liver microsomal preparations from human and mouse. Incubations (total volume 1.0 mL) were carried out at 37 °C for 60 min and contained 10 mM magnesium chloride, microsomal protein (2.0 mg/mL) or recombinant CYP1A2 (1 mg/mL), TBZ (50 μM) and 2.4 mM NADPH (prepared fresh) in 100 mM potassium phosphate buffer (pH 7.4). The TBZ stock solution was prepared in DMSO. The final concentration of DMSO in the incubation media was <0.2%. For detection of GSH conjugates, the incubations were fortified with reduced GSH (2 mM). Incubations that lacked NADPH, GSH or microsomes served as negative controls. All reactions were terminated

with 5 vol of acetonitrile. After centrifugation (3000g 10 min), the resulting supernatant was removed and evaporated to dryness under a steady stream of nitrogen. The residue was reconstituted in 30% acetonitrile in 0.1% formic acid (200 μL), vortex mixed and centrifuged. Aliquots (75 μL) of the final supernatant were analyzed by LC/MS.

Generation of the 5-OHTBZ Metabolite. 5-OHTBZ was generated by microsomal incubation of TBZ using the experimental conditions described above except that β-napthoflavone-treated rat liver microsomes (protein concentration 2 mg/mL) were used in the incubation mixture. After 45 min of incubation, additional NADPH (2 mM) was added to the incubation mixture to drive the reaction to completion. The reaction was stopped by addition of with ethyl acetate (3 mL) after 90 min and vortexed for 10 min. The mixture was then centrifuged and the ethyl acetate layer was separated and evaporated to dryness under a stream of N_2. The residue was reconstituted in mobile phase and analyzed by HPLC/MS to ensure the formation of 5-OHTBZ. The molecular ion and the retention time of the metabolite was compared to that of the authentic 5-OHTBZ (Dr. Ehrenstorfer GmBH, Augsburg, Germany) for confirming the formation of the metabolite. This crude 5-OHTBZ was used without further purification in subsequent liver microsomal or peroxidase incubations. A freshly prepared 5-OHTBZ sample was used for each of the incubations discussed below. An assessment of the yield of extracted 5-OHTBZ metabolite was made by comparing the peak area of the extracted material with that of the authentic 5-OHTBZ reference standard at 318 nm in the UV chromatogram and was estimated to be ~30% (15.4 nmol/mL).

Microsomal Incubation of 5-OHTBZ Metabolite. Dried ethyl acetate extract of the TBZ incubation (described above) containing 5-OHTBZ was reconstituted in a mixture containing phosphate buffer (100 mM, pH 7.4), $MgCl_2$ (10 mM), human or mouse liver microsomes (1 mg/mL), reduced GSH (2 mM) and NADPH (2 mM) in a final volume of 1.0 mL. After 60 min of

incubation at 37 °C, the mixture was processed as described previously and 75 μL aliquot of the reconstituted residue was analyzed by LC-MS/MS for the detection of GSH conjugate (M3).

Incubations of 5-OHTBZ with HRP. 5-OHTBZ was prepared as described above and resulting ethyl acetate extract was dried and reconstituted in a mixture containing phosphate buffer (100 mM, pH 7.4), HRP (2 units/mL), reduced GSH and/or reduced GSH-IP (5 mM) in a final volume of 1 mL. The reaction was initiated by addition of H_2O_2 (500 μM) and terminated after 30 min of incubation at 37 °C by addition of ascorbic acid solution (2 mM) followed by acetonitrile (5 mL) . The resulting mixture was centrifuged and the supernatant was dried under a steady stream of N_2 at 25 °C. The dried residue was reconstituted in a mixture of acetonitrile and 0.1% formic acid (30:70, 200 μL) and analyzed by LC-MS/MS. Incubations that lacked HRP enzyme or H_2O_2 served as negative controls.

Incubations of 5-OHTBZ with Ram Seminal Vesicle microsomes. Dried ethyl acetate extract containing 5-OHTBZ (prepared by the method described above) was reconstituted in phosphate buffer (100 mM, pH 7.4) containing ram seminal vesicle microsomes (1 mg/mL) and reduced GSH or GSH-IP (5 mM). Incubations were initiated with AA (300 μM) or H_2O_2 (500 μM). After 30 min of incubation at 37 °C, the reactions were terminated by addition of ascorbic acid (2 mM) followed by acetonitrile (5 mL). The samples were then processed and analyzed for the GSH or GSH-IP conjugates (M3 or M5), as described above. Incubations that lacked enzyme or the cofactors (H_2O_2 or AA) served as negative controls.

LC-MS/MS Analysis. The separation of metabolites was achieved at ambient temperature on a kromasil C4 100A column (3.5 μm, 150 x 2.0 mm, Phenomenex, Torrance, CA) by reverse phase chromatography. The mobile phase consisted of 0.1% formic acid (Solvent A) and acetonitrile (Solvent B) and was delivered at 0.200 mL/min. A gradient was used to separate the glutathione conjugates, metabolites and TBZ. The initial composition of solvent B was maintained at 1 % for 10 min and then increased in a linear manner as follows: 30% at 28 min;

50% at 30 min and 90% at 35 min. It was then maintained at 90% for up to 37 min and then decreased to 1% in the next 3 min. The column was allowed to equilibrate at 1% solvent B for 5 min prior to the next injection. The HPLC effluent going to the mass spectrometer was directed to waste through a divert valve for the initial 5 min after sample injection.

Mass spectrometric analyses were performed on a ThermoFinnigan Deca XP ion trap mass spectrometer, which was interfaced to an Agilent HP-1100 HPLC system (Agilent Technologies, Palo Alto, CA.) and equipped with an electrospray ionization source. The values for ESI were as follows: capillary temperature 270 °C; spray voltage 4.0 kV; capillary voltage 4.0 V; sheath gas flow rate 90 and auxillary gas flow rate 30. The mass spectrometer was operated in a positive ion mode with data-dependent scanning. The ions were monitored over a full mass range of *m/z* 125-1000. For a full scan, the automatic gain control was set at 5.0 x 10^8, maximum ion time was 100 ms and the number of microscans was set at 3. For MS^n scanning, the automatic gain control 1.0 x 10^8, maximum ion time was 400 ms and the number of microscans was set at 2. For data dependent scanning, the default charge-state was 1, default isolation width was 3.0, normalized collision energy was 45.0.

Isolation of GSH-IP conjugate (M5) and ^{1}H NMR Analysis. GSH-IP conjugate (M5) was generated using HRP by the method described above and separated by HPLC on an Aqua C18 column (5 um, 150 x 4.6 mm, Phenomenex, Torrance CA). The product was eluted using a linear gradient starting with acetonitrile at 10% and 0.1% formic acid (90%) and ramped to 70% acetonitrile over 20 minutes at a flow rate of 1 mL/min. Fractions were collected every 30 seconds throughout the run. The pooled fractions were evaporated to dryness, reconstituted in mobile phase and again subjected to HPLC separation using the same column but under isocratic conditions (mobile phase of 0.1% formic acid:acetonitrile, 88 :12). Fractions containing M5 were collected, combined and evaporated under N_2 using a Speed Vac concentrator. The fractions contained no detectable free unreacted GSH-IP. The residue was reconstituted in deuterated methanol for NMR experiments and a sample (10 μL) was analyzed by LC-MS/MS

to examine its purity. ^{1}H and 2D COSY NMR spectra were recorded at 30 °C on a 700 MHz Bruker-Biospin AV700 spectrometer equipped with a 5 mm TCI z-gradient Cryoprobe. ^{1}H NMR data were acquired with water suppression using a Watergate W5 pulse sequence with gradients and a double echo. ^{1}H ^{1}H COSY NMR data were acquired without solvent suppression using gradient pulses for coherence selection. Data processing was performed using the XWINNMR 3.5 software package (Bruker-Biospin). Chemical shifts were referenced to an internal standard of tetramethylsilane.

DMD Fast Forward. Published on January 24, 2006 as DOI: 10.1124/dmd.105.008094
This article has not been copyedited and formatted. The final version may differ from this version.

Results

Metabolism of TBZ by Human and Mouse Liver Microsomes. Metabolism of TBZ was studied in human and mouse liver microsomes to compare the metabolic profile of the compound in the two species. Mouse was chosen since most TBZ toxicities were observed in this species. Fig. 2 shows the total ion and UV chromatograms of extracts from incubation of TBZ with NADPH-supplemented human liver microsomes. The total ion chromatogram showed one major peak (5-OHTBZ) at 22 min that gave a protonated molecular ion at *m/z* 218, in addition to the peak corresponding to unchanged TBZ at 24 min (*m/z* 202). A minor peak (DiOHTBZ) was also detected in the chromatogram at a retention time of 21 min with a protonated molecular ion at *m/z* 234. The metabolic profile of TBZ following incubations with mouse liver microsomes was similar to that in humans except that DiOHTBZ was not observed in the mouse. Incubation of TBZ with recombinant CYP1A2 also resulted in the formation of 5-OHTBZ as the primary metabolite (data not shown). This result was consistent with previous reports on TBZ metabolism in liver microsomes and hepatocytes of humans and preclinical species (Coulet et al., 1998a; Coulet et al., 1998b). The TBZ peak at 24 min gave a protonated molecular ion at *m/z* 202 with primary fragment ions at *m/z* 175 and 132 (Fig. 3A). Both the fragment ions resulted from the cleavage of the thiazole moiety in the molecule. The product ion mass spectrum of 5-OHTBZ at *m/z* 218 showed a fragment ion at 191 amu (Fig. 3B) that was 16 amu greater than the base fragment ion at *m/z* 175 in the TBZ mass spectrum. This was consistent with hydroxylation of benzimidazole moiety of TBZ. The NMR spectrum of crude 5-OHTBZ showed a change in the pattern in the aromatic region with the disappearance of proton e at position 5 when compared to the NMR spectrum of TBZ (Table 1). The new pattern showed two doublets (J = 9.0 *Hz*) at 7.5 and 6.83 ppm, which was assigned to the protons c and d at positions 6 and 7 and a doublet at 7.3 ppm that was assigned to the proton f at position 4. The identity of 5-OHTBZ was further confirmed by comparison of its MS spectra and

DMD Fast Forward. Published on January 24, 2006 as DOI: 10.1124/dmd.105.008094
This article has not been copyedited and formatted. The final version may differ from this version.

retention time to that of the authentic 5-OHTBZ. The minor peak, DiOHTBZ, on the other hand gave fragment ions that were consistent with dihydroxylated thiabendazole (data not shown).

Formation of GSH Conjugate of 5-OHTBZ (M3) by Human and Mouse Liver Microsomes. LC/MS/MS analysis of NADPH-supplemented human or mouse liver microsomal and recombinant CYP1A2 incubations containing TBZ and reduced GSH afforded only one adduct (M3) (R_t = ~20 min) with a molecular ion (MH^+) at 523 (Fig. 4A). All incubations produced the same adduct as observed from its retention time and the molecular weight. The product ion mass spectrum of M3 produced fragment ions at *m/z* 505, 394 and 250 (Fig. 4B). The fragment ion *m/z* 394 indicated a loss of 129 amu from the molecule and corresponded to loss of the pyroglutamate moiety, which is characteristic of a glutathione conjugate (Baillie and Davis, 1993). The fragment ion at *m/z* 250 was assigned as a cleavage adjacent to cysteinyl thioether moiety with the charge retention on the hydroxythiabendazole moiety (Fig. 4B).

Incubation of 5-OHTBZ with human or mouse liver microsomes and recombinant CYP1A2 containing NADPH and reduced GSH, also afforded the same GSH conjugate as that produced in the incubations with TBZ (data not shown). Although the synthetic standard of 5-OHTBZ was available, it was expensive and very difficult to obtain. Therefore, 5-OHTBZ was generated by incubation of TBZ with hepatic microsomes in this study. The formation of 5-OHTBZ is mainly catalyzed by CYP1A2 (Coulet et al., 1998b) therefore, β-napthoflavone treated rat liver microsomes were used to produce this metabolite from TBZ as described in the methods section. This procedure yielded about 30% of the 5-OHTBZ (after extraction with ethyl acetate). The total ion chromatogram and the UV chromatogram of the extracted material showed only one peak suggesting that the extracts were free of unreacted TBZ. Further, the molecular ion and the retention time of this peak coincided with the retention time and the molecular ion of the authentic standard of 5-OHTBZ further confirming the structure of the metabolite. Since the focus of this study was to identify the glutathione conjugate of 5-OHTBZ, extracted 5-OHTBZ

was used without further purification for all incubations. The formation of M3 was not observed in control incubations lacking NADPH or reduced GSH, thus implicating the involvement of P450 in its formation.

Formation of GSH Conjugate of 5-OHTBZ (M3) by HRP. LC-MS/MS analysis of the mixture following incubation of extracted 5-OHTBZ with the HRP/H_2O_2/GSH system resulted in a GSH conjugate that had the retention time, molecular ion, and MS/MS fragmentation pattern identical to M3 formed in P450-mediated incubations (Fig. 5A). This peak was absent when H_2O_2 or HRP was lacking from the incubation mixture. TBZ was also incubated with HRP (2 units), H_2O_2 and reduced GSH as a control (data not shown). This incubation also lacked M3, suggesting that presence of 5-OHTBZ was necessary for its formation.

In addition to M3, HRP-mediated incubations also resulted in another product (M4) that gave a protonated molecular ion of *m/z* 433 in the LC/MS analysis (Fig. 5B). The product ion of *m/z* 433 produced fragment ions at *m/z* 406, 218 and 191 (Fig. 5C). The fragment ion at *m/z* 406 indicated a loss of 27 amu, which was similar to that observed in the product ion spectra of TBZ and 5-OHTBZ (Fig. 3). The major ion at *m/z* 218 and 191 suggested a cleavage of M4 to the 5-OHTBZ moiety and a subsequent loss of 27 amu as observed before (Fig. 3). Together, this data suggested that M4 was a dimer of 5-OHTBZ.

Formation and Structural Characterization of GSH-IP conjugate of 5-OHTBZ (M5) Using ^{1}H NMR and ^{1}H-^{1}H COSY NMR Analysis. Since M3 was produced in reasonably high amounts in the HRP-mediated oxidations, this source was used to generate sufficient quantities of M3 for NMR experiments. However, repurification of M3 proved to be extremely difficult (probably owing to high polarity of the conjugate). Therefore, reduced GSH was substituted with GSH-IP (the isopropyl functionality imparted enough nonpolarity and retention). The isopropyl ester derivative also helped in improving the sensitivity in conjugate detection relative to the free

carboxylic acid analog. This was consistent with previous reports by Soglia (Soglia et al., 2004) that showed a similar increase in sensitivity on using an ethyl ester of reduced GSH.

Incubations of 5-OHTBZ with the HRP/H_2O_2 system and containing GSH-IP gave the corresponding GSH-IP conjugate, M5, with a retention time of 25 min (Fig. 6A). LC-MS/MS analysis of M5 gave a molecular ion at *m/z* 565, which was 42 amu greater than the molecular ion of M3 (*m/z* 523). The MS/MS spectrum of M5 gave fragment ions at *m/z* 436 and 250 (Fig. 6B). The ion at *m/z* 436 was 42 amu greater than *m/z* 394 and the ion at *m/z* 250 was similar to that observed in MS/MS spectrum of M3 (Fig. 4B).

Repurified M5 was found to be free of detectable unreacted GSH-IP and suitable for NMR experiments. ^{1}H NMR and ^{1}H ^{1}H COSY experiments were performed by dissolving M5 in deuterated methanol and allowed confirmation of the structure of GSH-IP adduct. The key change in the ^{1}H NMR spectrum of M5 was the disappearance of the resonance signal at 7.3 ppm for proton f at the 4-position of 5-OHTBZ (Table 1). This was consistent with the addition of the GSH-IP moiety at the 4 position of 5-OHTBZ. Other resonances in the spectrum (between 1 and 5 ppm, Table 1) coincided with the protons of the GSH-IP moiety. Correlation of the protons, c and d, in the ^{1}H ^{1}H COSY NMR spectrum further confirmed the position of attachment of GSH-IP to 5-OHTBZ (see supplemental material).

Two additional peaks (M6/M7, R_t = 27.2 and 28 min) with protonated molecular ion at *m/z* 912 were also detected in the total ion chromatogram when 5-OHTBZ was incubated with HRP, H_2O_2, and reduced GSH-IP (Fig. 7A). The MS/MS spectra of both peaks at *m/z* 912 were similar and showed major fragment ions at *m/z* 783 and 654 corresponding to losses of one and two pyroglutamate moieties, respectively (Fig. 7B). This suggested that the products were GSH-IP adducts of 5-OHTBZ in which two molecules of reduced GSH-IP were added to one

molecule of 5-OHTBZ. The position of the second GSH-IP molecule was not discernible from the spectrum.

Formation of GSH Conjugate (M3) or GSH-IP conjugate (M5) by Ram Seminal Vesicle Microsomes. Ram seminal vesicle (RSV) microsomes, which contain a high activity of PGS (Marnett et al., 1983), were used as a source of PGS. The peroxidase activity in the RSV microsomes was determined to be 5.4 μmol/min/mg of protein, using guaiacol as a substrate as described previously (Kalgutkar and Marnett, 1994). RSV microsomal incubations of 5-OHTBZ were fortified with reduced GSH (or GSH-IP) and initiated with either arachidonic acid or H_2O_2 (to bypass the cyclooxygenase step of PGS). An extracted ion chromatogram of these incubation mixtures (Fig. 8) also showed the formation of M3 and M5 with reduced GSH and GSH-IP, respectively and the dimer M4, suggesting that PGS mediated oxidation of 5-OHTBZ afforded the same products as those generated by HRP. The oxidation of 5-OHTBZ occurred during the peroxidase portion of the enzyme reaction since both arachidonic acid and H_2O_2 were capable of supporting this oxidation. The controls that did not contain arachidonic acid or H_2O_2 lacked M3, M4 and M5.

Discussion

The potential of 5-OHTBZ, a major metabolite of TBZ, to undergo metabolic activation by P450 and peroxidases was explored in this study. In vitro conjugation with glutathione is a commonly used model to establish the presence of reactive metabolites and probe metabolic activation. This method was used to trap the reactive metabolites of 5-OHTBZ in the current study. Identification of the GSH conjugate of 5-OHTBZ (M3) in incubations of TBZ with NADPH and GSH supplemented hepatic microsomes or recombinant CYP1A2, clearly indicated an alternative P450-catalyzed mechanism of bioactivation of TBZ in addition to the previously reported thiazole cleavage mechanism. Although the precise mechanism was not definitively established, the absence of other GSH conjugates in the incubation mixtures suggested that M3 was formed by P450-catalyzed 2-electron oxidation of 5-OHTBZ followed by nucleophilic attack of reduced GSH on the resulting quinone imine **1** (Scheme 1). This was further confirmed when incubations of isolated 5-OHTBZ with NADPH and GSH supplemented liver microsomes afforded the same GSH adduct M3, as observed in TBZ supplemented incubations. Two-electron oxidation of phenols by P450 has been previously documented (Testa, 1995). Previous studies on P450-mediated acetaminophen bioactivation have also suggested a similar mechanism for acetaminophen conversion to *N*-acetyl-*p*-benzoquinone imine (Potter and Hinson, 1987a). Attempts to isolate or characterize the quinone imine intermediate of 5-OHTBZ by LC-MS/MS failed and this was attributed to its instability.

Incubations of 5-OHTBZ with HRP or microsomal PGS also produced M3 when GSH was present in the media. This suggested that 5-OHTBZ was also metabolized by peroxidases. Furthermore, the presence of M3 in RSV microsomal incubations containing H_2O_2 indicated that hydroperoxidase activity of PGS catalyzes this oxidation. HRP is a non-specific one-electron oxidant that is widely used in analogous studies of oxidative bioactivation of endogenous and

DMD Fast Forward. Published on January 24, 2006 as DOI: 10.1124/dmd.105.008094
This article has not been copyedited and formatted. The final version may differ from this version.

foreign compounds, especially phenols and aromatic amines (Potter and Hinson, 1987, Smith et al., 2003). In light of the nephrotoxicity and teratogenicity observed following TBZ administration, PGS was selected as a mammalian model enzyme to probe the oxidative metabolism of 5-OHTBZ. PGS is a microsomal hemoprotein that catalyzes the oxidation of arachidonic acid to prostaglandin H_2 (PGH_2) in reactions which utilize both cyclooxygenase and peroxidase activities (O'Brien, 2000; Vogel, 2000; Smith et al., 1991). During this process, the enzyme activities generate enzyme and substrate-derived free radicals that can simultaneously co-oxidize numerous xenobiotics. If not detoxified, these reactive intermediates can oxidize and/or covalently modify DNA and proteins. PGS is present in high concentrations in the kidney (Moldeus et al., 1982; Potter and Hinson, 1987b; Lock and Reed, 1998). Immunohistochemical localization studies have also revealed the presence of PGS in high activity in mouse embryos (Kulkarni, 2001; Paman et al., 1999).

Detection of the dimer M4 of 5-OHTBZ in peroxidase-mediated incubations was consistent with the previous reports on oxidation of phenolic substrates with peroxidases (Potter and Hinson, 1987a; Thompson et al., 1989). A mechanism similar to that described for the oxidation of acetaminophen by HRP and PGS was therefore proposed for the oxidation of 5-OHTBZ and is shown in Scheme 2. The peroxidase-catalyzed one electron oxidation of 5-OHTBZ would produce a phenoxy radical (**2**). This radical could rearrange to the corresponding carbon centered phenyl radical **3** that could dimerize to M4. Alternatively, a disproportionation reaction between two molecules of **3** or a sequential peroxidase-mediated single electron oxidation of **2** (Bessems et al., 1998) can afford the quinone imine like species (**1**), which on reaction with GSH or GSH-IP can afford M3 or M5, respectively. Since the identity of GSH conjugate formed by P450 and peroxidase was the same (based on the retention time and MS/MS spectra), it was reasonable to assume that 5-OHTBZ was activated to the same reactive intermediate by both enzyme systems.

As mentioned before, GSH-IP was used for further characterization of the GSH adduct, M5, by NMR. Since GSH-IP was only an isopropyl derivative of reduced GSH, it was conceivable that the site of attack by reduced GSH to form M3 would be the same as in M5. Although three sites were available in **1** for nucleophilic attack by GSH, actual structural assignment by NMR suggested the addition of GSH-IP at the 4-position of 5-OHTBZ. This was probably due to extended charge delocalization in the intermediate and greater electronegativity of oxygen relative to that of nitrogen. Furthermore, the attack at the 4 position of **1** was probably attributed to greater electrophilicity of the C4 position, which is flanked by the carbonyal group and an electronegative sp^2 nitrogen (imine functionality of benzimidazole) compared to position 6.

A bis-conjugate (M6/M7), in which two molecules of GSH-IP were added to 5-OHTBZ, was also detected in the peroxidase-mediated incubations (Scheme 2). Previous studies have demonstrated that introduction of cysteinyl groups into the molecule decreases its redox potential and these molecules undergo redox cycling to produce reactive oxygen species more readily than quinone imines (Lindqvist et al., 1991). A similar conclusion could be made in this study. Thus, formation of M5 made it even more prone to oxidation and susceptible to a nucleophilic attack by second GSH-IP molecule. It is possible that this potential of the GSH conjugate to readily oxidize can increase, rather than decrease, the toxic effects of quinone imines by stressing the endogenous thiol pool and depleting cellular GSH. Since the bis-conjugate was formed in smaller amounts, no attempt was made to isolate and characterize it. Hence the exact position of addition of the second GSH-IP group could not be determined.

In conclusion, this study provides evidence that 5-OHTBZ can undergo oxidation by P450 and peroxidases to an electrophilic species that can be trapped by GSH. The results also support the role of 5-OHTBZ in the toxicity of TBZ that have been previously postulated by Coulet and co-workers (Coulet et al., 2000). The reaction of activated 5-OHTBZ with thiols could be of biological significance especially since TBZ administration has been shown to increase the

depletion of renal and hepatic GSH in vivo (Mizutani et al., 1990). Although the in vivo relevance of 5-OHTBZ activation by peroxidases and/or P450 and the GSH conjugate formation is not established in this study, the results provide some indication that TBZ-induced toxicities observed in animals and humans could partially be due to peroxidase and/or P450-mediated bioactivation of 5-OHTBZ, in addition to the well-documented thiazole cleavage.

References

Baillie TA, and Davis AR (1993) Mas spectrometry in the analysis of glutathione conjugates. *Biol. Mass Spectrom.* **22**: 319-325.

Bauer LA, Raisys VA, Watts MT, and Ballinger J (1982) The pharmacokinetics of thiabendazole and its metabolitesin an anepheric patient undergoing hemodialysis and hemoperfusion. *J. Clin. Pharmacol*. **22**:276-280.

Bessems JGM, de Groot MJ, Baede JM, Te Koppele JM, and Vermeulen NPE (1998) Hydrogen atom abstraction of 3,5-disubstituted analogues of paracetaml by horse radish peroxidase and cytochrome P450. *Xenobiotica* **28**:855-875.

Bion E, Pariente AP, and Maitre F (1995) Severe cholestasis and sicca syndrome after thiabendazole. *J. Hepatol*. **23**:762-763.

Coulet M, Eeckhoutte C, Larrieu G, Sutra J–F, Hoogenboom LAP, Huveneers-Oorsprong MBM, Kuiper HA, Castell JV, Alvinerie M, and Galtier P (1998a) Comparative metabolism of thiabendazole in cultured hepatocytes from rats, rabbits, calves, pigs, and sheep, including the formation of protein bound residues. *J. Agri. Food. Chem*. **46**:742-748.

Coulet M, Dacasto M, Eeckhoutte C, Larrieu G, Sutra JF, Alvierie M, Macé K, Pfeifer AMA., and Galtier P (1998b) Identification of human and rabbit cytochrome P4501A2 as major isoforms involved in thiabendazole 5-hydroxylation *Fundam. Clin. Pharmacol*. **12**:225-235.

Coulet M, Dacasto M, Eeckhoutte C, Larrieu G, Sutra JF, Alvierie M, Macé K, Pfeifer AMA, Zucco F, Stammati AL, De Angelis I Vignoli AL, and Galtier P (2000) Evidence for cytochrome P4501A2 mediated protein covalent binding of thiabendazole and for its passive

intestinal transport: use of human and rabbit derived cells. *Chem. Biol. Interact*. **127**:109-124.

Fujitani T, Tada Y, and Yoneyama M (1999) Effects of thiabendazole (TBZ) on mitochondrial function in renal cortex of ICR mice. *Food Chem. Toxicol*. **27**:307-315.

Fujitani T, Yoneyyama M, Ogata A, Ueta T, Mori K, and Ichikawa H (1991) New metabolites of thiabendazole and the metabolism of thiabendazole by mouse embryo in vivo and in vitro. *Food Chem. Toxicol*. **29**:265-274.

Groten JP, Butler W, Feron VJ, Kozianowski G, Renwick AG, and Walker R (2000) An analysis of the possibility for health implications of joint actions and interactions between food additives. *Reg. Toxicol. Pharmacol*. **31**:77-91.

Kalgutkar AS, and Marnett LJ (1994) Rapid inactivation of prostaglandin endoperoxide synthases by N-(carboxyalkyl)maleimides. *Biochemistry* **33**:8625-8628.

Kulkarni AP (2001) Role of biotransformation in conceptual toxicity of drugs and other chemicals. *Curr. Pharm. Des*. **7**:833-857.

Lindqvist T, Kenne L, and Lindeke B (1991) On the chemistry of the reaction between N-acetylcysteine and 4-[(4-ethoxyphenyl)imino]-2,5-cyclohexadien-1-one, a 4-ethoxyanailine metabolite formed during peroxidase reactions. *Chem. Res. Toxicol*. **4**:489-496.

Lock EA, and Reed CJ (1998) Xenobiotic metabolizing enzymes of the kidney. *Toxicol. Pathol*. **26**:18-25.

Manivel JC, Bloomer JR, and Snover DC (1987) Progressive bile duct injury after thiabendazole administration. *Gastroenterology* **93**:245-249.

Marnett LJ, Dix TA, Sachs RJ and Siedlik PH (1983) Oxidations by fatty acid hydroperoxides and prostaglandin synthase, in, *Advances in Prostaglandins, Thromboxanes, and Leukotriene Research* (Samuelsson B, Paoletti R, and Ramwell P, eds.) vol 11 pp 79-86, Raven Press, New York.

Mizutani T, Ito K, Nomura H, and Nakanishi K (1990) Nephrotoxicity of thiabendazole in mice depleted of glutathione by treatment with DL-buthionine sulphoximine. *Food Chem. Toxicol.* **28**:169-177.

Mizutani T, Yoshida K, and Kawazoe S (1994) Formation of toxic metabolites from thiabendazole and other thiazoles in mice. Identification of thioamides as ring cleavage products. *Chem. Res. Toxicol*. **22**:750-755.

Moldéus P, Andersson B, Rahimtula A, and Berggren M (1982) Prostaglandin synthetase catalyzed activation of paracetamol. *Biochem. Pharmacol*. **31**:1363-1368.

Monks TJ, and Jones DC (2002) The metabolism and toxicity of quinones, quinoneimines, quinone methides, and quinone-thioethers. *Curr. Drug Metab*. **3**:425-438.

O'Brien P (2000) Peroxidases *Chem. Biol. Interact*. **129**:111-139.

Ogata A, Ando H, Kubo Y, and Hiraga K (1984) Teratogenicity of thiabendazole in ICR mice. *Food and Chem. Toxicol*. **22**:509-520.

Parman T; Wiley MJ, and Wells PG (1999) Free radical mediated oxidative DNA damage in the mechanism of thalodimide teratogenicity. *Nat. Med*. **5**:582-585.

Potter DW and Hinson JA (1987a) Mechanisms of acetaminophen oxidation to N-acetyl-p-benzoquinone imine by horseradish peroxidase and cytochrome P450. *J. Biol. Chem*. **262**:966-973.

Potter DW, and Hinson JA (1987b) The 1- and 2-electron oxidation of acetaminophen catalyzed by prostaglandin synthase. *J. Biol. Chem*. **262**:974-980.

Rey-Grobellet X, Eeckhoutte C Sutra JF, Alvinerie M, and Galtier P (1996) Major involvement of rabbit liver cytochrome P4501A in thiabendazole 5-hydroxylation. *Xenobiotica* **26**:765-778.

Smith B J, Curtis JF, and Eling TE (1991) Bioactivation of xenobiotics by prostaglandin H synthase. *Chem. Biol. Interact*. **79**:245-264.

Smith KS, Smith PL, Heady TN, Trugman JM, Harman WD, and MacDonald TL In vitro metabolism of tolcapone to reactive intermediates: Relevance to tolcapone liver toxicity. (2003) *Chem. Res. Toxicol*. **16**:123-128.

Soglia JR, Harriman SP, Zhao S, Barberia J.; Cole MJ, Boyd JG, and Contillo LG (2004) The development of a higher throughput reactive intermediate screening assay incorporating micro-bore liquid chromatography-micro-electrospray ionization-tandem mass spectrometry and glutathione ethyl ester as an in vitro conjugating agent. J*. Pharm. and Biomed. Anal*. **36**:105-116.

Tada Y, Fujitani T, and Yoneyama M (1992) Acute renal toxicity of thiabendazole (TBZ) in ICR mice. *Food Chem. Toxicol.* **30**:1021-1030.

Testa B 1995 Monooxygenase catalyzed oxidation of oxygen and sulfur containing compounds, in *Metabolism of Drugs and Xenobiotics* pp 235-283, Academic Press, San Diego.

Thompson DC, Cha Y-N, and Trush MA (1989) The peroxidase-dependent activation of butylated hydroxyanisole and butylated hydroxytoluene to reactive intermediates. *J. Biol. Chem*. **264**:3957-3965.

Tocco DJ, Rosenblum C, Martin CM, and Robinson HJ (1966) Absorption, metabolism, and excretion of thiabendazole in man and laboratory animals. *Toxicol. Appl. Pharmacol*. **9**:31-39.

Tsuchiya T, Tanaka A, Fukukoa M, Sato M, and Yamaha T (1987) Metabolism of thiabendazole and teratogenic potential of its metabolites in pregnant mice. *Chem. Pharm. Bull*. **35**:2985-2993.

Vogel C (2000) Prostaglandin H synthases and their importance in chemical toxicity. *Curr. Drug Metab*. **1**:391-404.

Walton K, Walker R, van de Sandt JJM, Castell JV, Knapp AGAA, Kozianowski G, Roberfroid M, Schilter B (1999) The application of in vitro data in the derivation of the acceptable daily intake of food additives. *Food Chem. Toxicol*. **37**:1175-1197.

Wilson CG, Parke DV, Cawthrone MA (1973) 5-Hydroxylation of thiabendazole in rat liver microsomal preparations. *Biochem. Soc. Trans.* **1**:195-196.

Yoneyama M, and Ichikawa H (1986) Irreversible in vivo and in vitro binding of thiabendazole to tissue proteins of pregnant mice. *Food Chem. Toxicol*. **24**:1283-1286.

Figure Legends

Figure 1. Structures of Thiabendazole (TBZ), Thioformamide, Acetaminophen and 5-Hydroxythiabendazole (5-OHTBZ).

The mechanism for the formation of thioformamde has been depicted previously (Mizutani et al. 1994).

Figure 2. Total ion and UV chromatogram following incubation of TBZ with NADPH-supplemented human liver microsomes.

The total ion chromatogram following incubation of TBZ (50 μM) with NADPH-supplemented mouse liver microsomes was similar to that of human liver microsomes except that DiOHTBZ was not detected in mouse liver microsomal incubations.

Figure 3. Product ion mass spectra of A) TBZ at *m/z* 202 ($M+H^+$) and B) 5-OHTBZ at *m/z* 218 ($M+H^+$) obtained by CID of the parent ion in NADPH-supplemented human liver microsomes. The origins of the characteristic ions are indicated.

Figure 4. Extracted ion chromatogram (A) and MS/MS spectrum (B) obtained by CID of the parent ion of the GSH conjugate of 5-OHTBZ (M3), at *m/z* 523 ($M+H^+$) at R_t = 20 min following incubation of TBZ with NADPH-supplemented human liver microsomes in the presence of reduced GSH.

GSH conjugate (M3) was formed when isolated 5-OHTBZ was incubated with human liver microsomes in the presence of NADPH and reduced GSH. Incubation of TBZ with mouse liver microsomes, NADPH, and reduced GSH also resulted in M3.

Figure 5. Extracted ion chromatogram of (A) GSH conjugate of 5-OHTBZ M3, (*m/z* 523), (B) dimer M4, and (C) MS/MS spectrum obtained by CID of the parent ion ($M+H^+$) at *m/z* 433 (R_t =

16.5 min) following incubation extracted 5-OHTBZ with HRP (2 units) in the presence of GSH and H_2O_2.

The signal of 5-OHTBZ completely disappeared on its incubation with HRP.

Figure 6. Extracted ion chromatogram of the GSH-IP conjugate of 5-OHTBZ M5, (A) (R_t 24.5 min) and MS/MS spectrum (B) of the parent ion of M5 at *m/z* 565 following incubation of 5-OHTBZ with HRP and H_2O_2 in the presence of reduced GSH-IP.

Daughter ions resulting from GSH-IP cleavage such as loss of pyroglutamic acid ($[MH-129]^+$) are as indicated.

Figure 7. Extracted ion chromatogram of GSH-IP bis-conjugates of 5-OHTBZ M6/M7 (A) (R_t 27.2 and 28 min) and MS/MS spectrum (B) of parent ion of M6/M7 at *m/z* 912 following incubation of 5-OHTBZ with HRP and H_2O_2 in the presence of reduced GSH-IP.

Daughter ions resulting from GSH-IP cleavage such as loss of one or both pyroglutamic acids ($[MH-129]^+$) are as indicated.

Figure 8. Extracted ion chromatogram of GSH conjugate of 5-OHTBZ M3 (A) and the dimer M4 (B) following incubation of extracted 5-OHTBZ with RSV microsomes (1 mg/mL protein concentration) in the presence of GSH and arachidonic acid.

Schemes

Scheme 1. Proposed pathway for the formation of GSH conjugates M3, from TBZ or 5-OHTBZ in microsomal incubations supplemented with NADPH and GSH.

Shown is the formation of quinone-imine (**1**) followed by a nucleophilic attack of GSH at the 4-position of 5-OHTBZ.

Scheme 2. Proposed pathway for the formation of GSH conjugates M3, M5, and the dimer M4 via the arachidonic acid mediated PGS catalyzed (A) or H_2O_2 mediated HRP catalyzed (B) oxidation of 5-OHTBZ.

DMD Fast Forward. Published on January 24, 2006 as DOI: 10.1124/dmd.105.008094
This article has not been copyedited and formatted. The final version may differ from this version.

Table 1. ^{1}H NMR Spectroscopy Data for Thiabendazole (TBZ), 5-Hydroxythiabendazole (5-OHTBZ) and 4-Isopropyloxyglutathionyl-5-hydroxy-thiabendazole (M5).

ND - The chemical shift for resonance signal for the protons i in the NMR spectrum of coincided with the resonance signal of water molecule and hence was not observed.

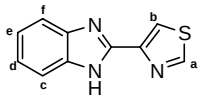

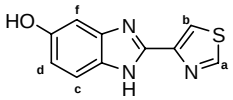

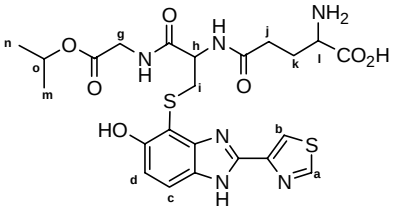

Proton	Chemical Shift (ppm)	J (*Hz*)	Chemical Shift (ppm)	J (*Hz*)	Chemical Shift (ppm)	J (*Hz*)
a	9.15 (d, 1H)	2.01	9.2 (d, 1H)	2.01	9.15 (s, 1H)	
b	8.23 (d, 1H)	2.01	8.25 (d, 1H)	2.01	8.37 (s, 1H)	
c	7.30 (m, 4H)		7.5 (d, 1H)	9.0	7.51 (d, 1H)	9.0
d			6.83 (d, 1H)	9.0	6.94 (d, 1H)	9.0
e						
f			7.3 (d)			
g					4.56 (s, 2H)	
h					3.95 (m, 1H)	
i					ND	
j					2.51 (m, 2H)	
k					2.06 (m, 2H)	
l					3.55 (t, 1H)	7.0
m					1.10 (d, 6H)	6.0
n						
o					3.8 (m, 1H)	6.0

ND – masked by resonance signals from water

Figure 1

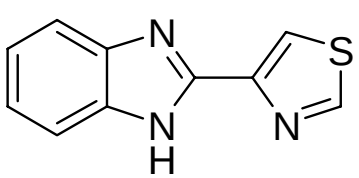

Thiabendazole (TBZ)

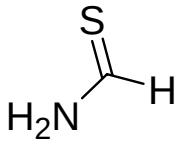

Thioformamide

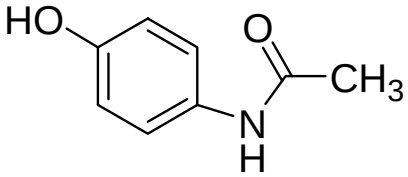

Acetaminophen

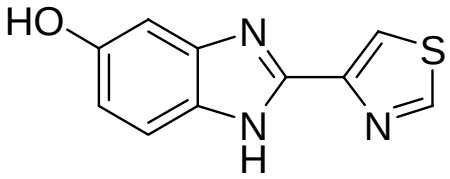

5-Hydroxythiabendazole (5-OHTBZ)

Figure 2

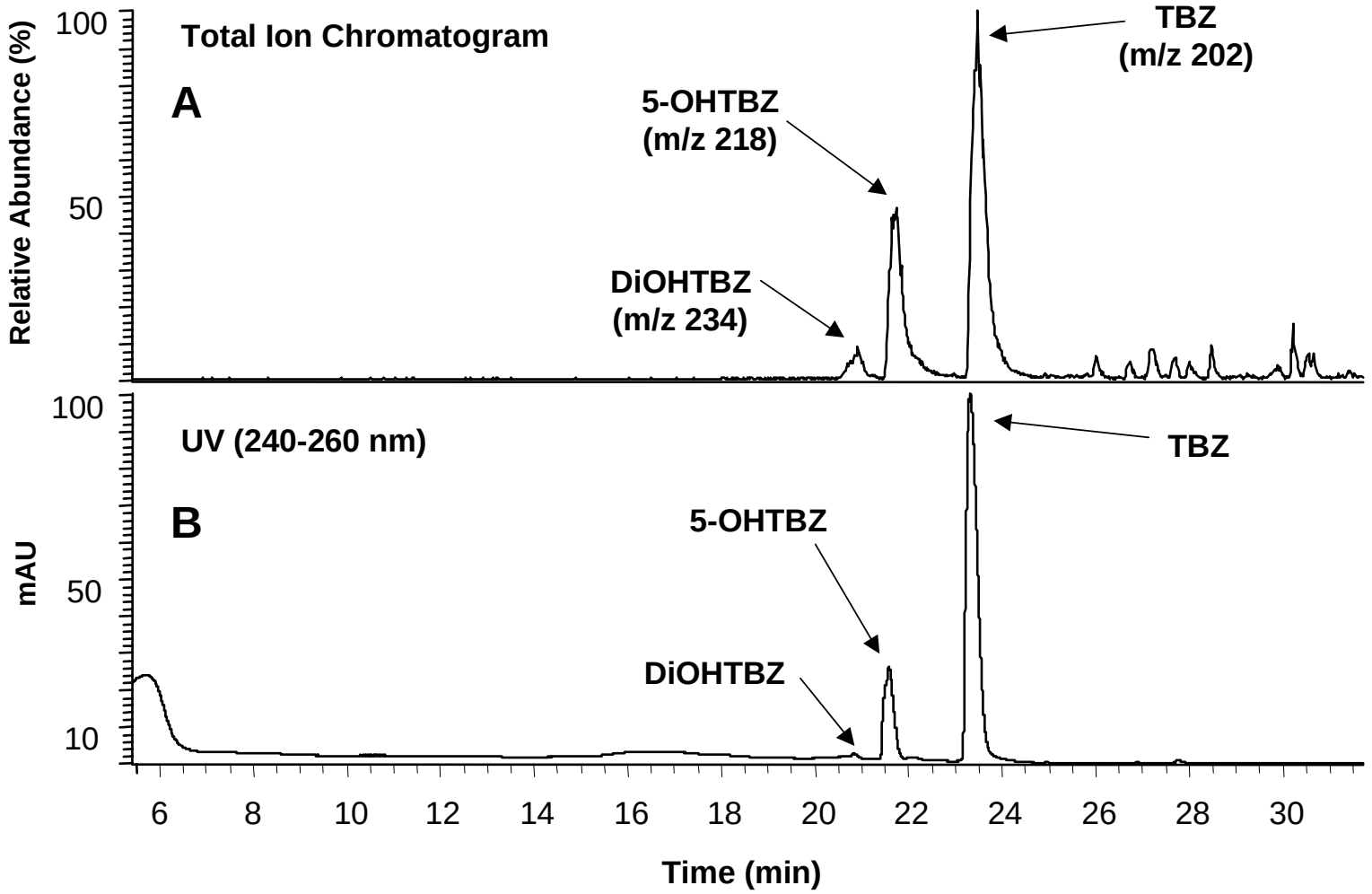

Figure 3

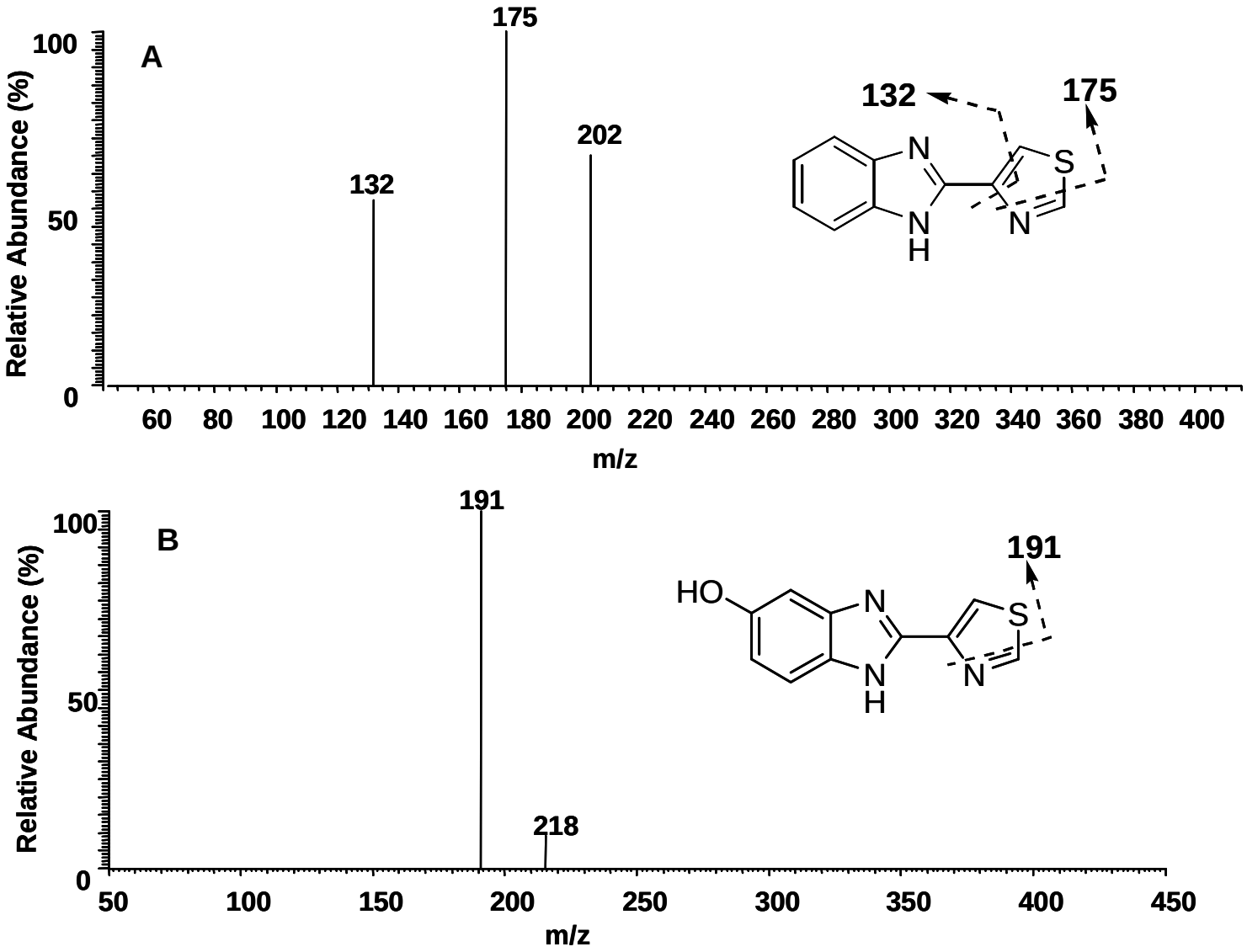

Figure 4

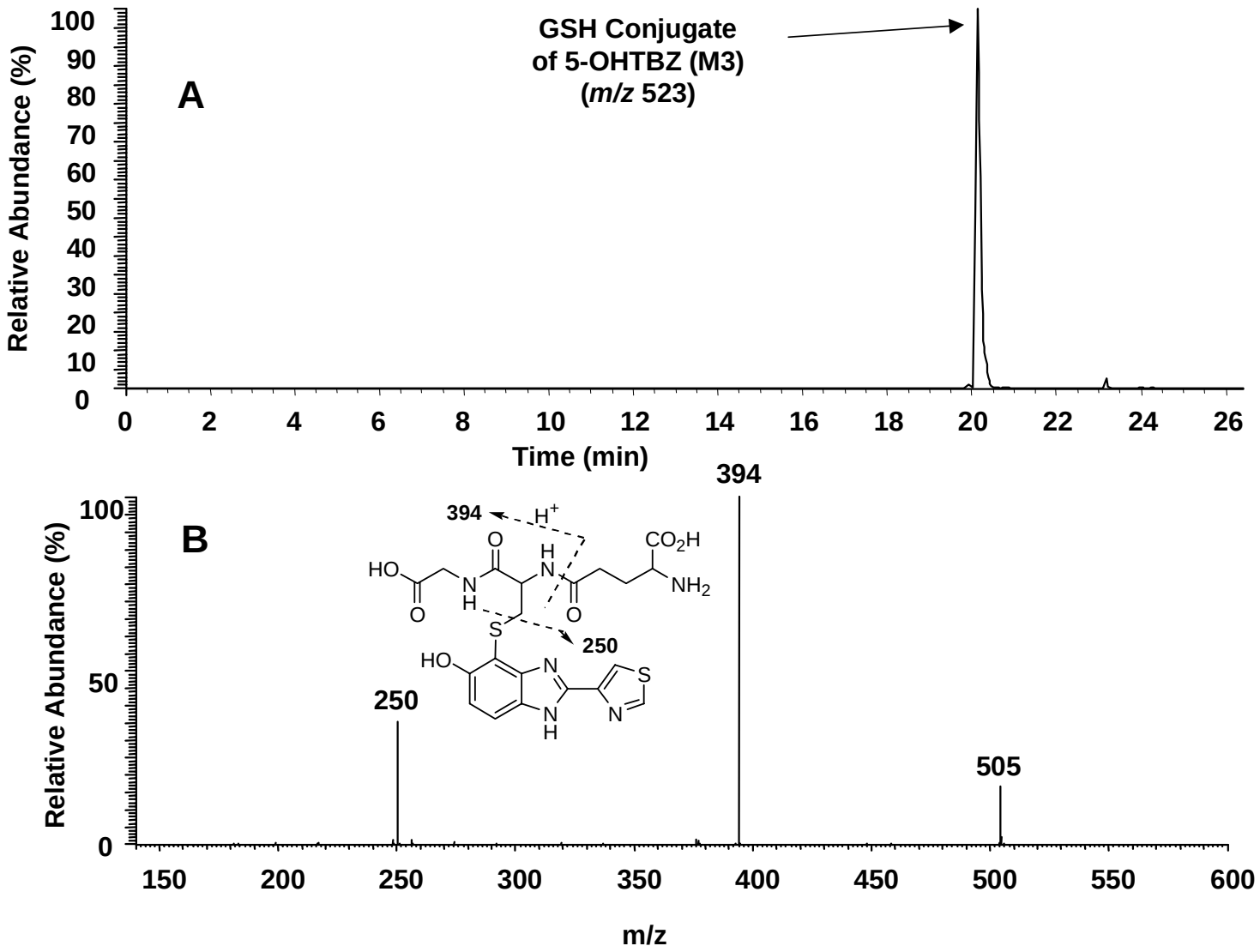

Figure 5

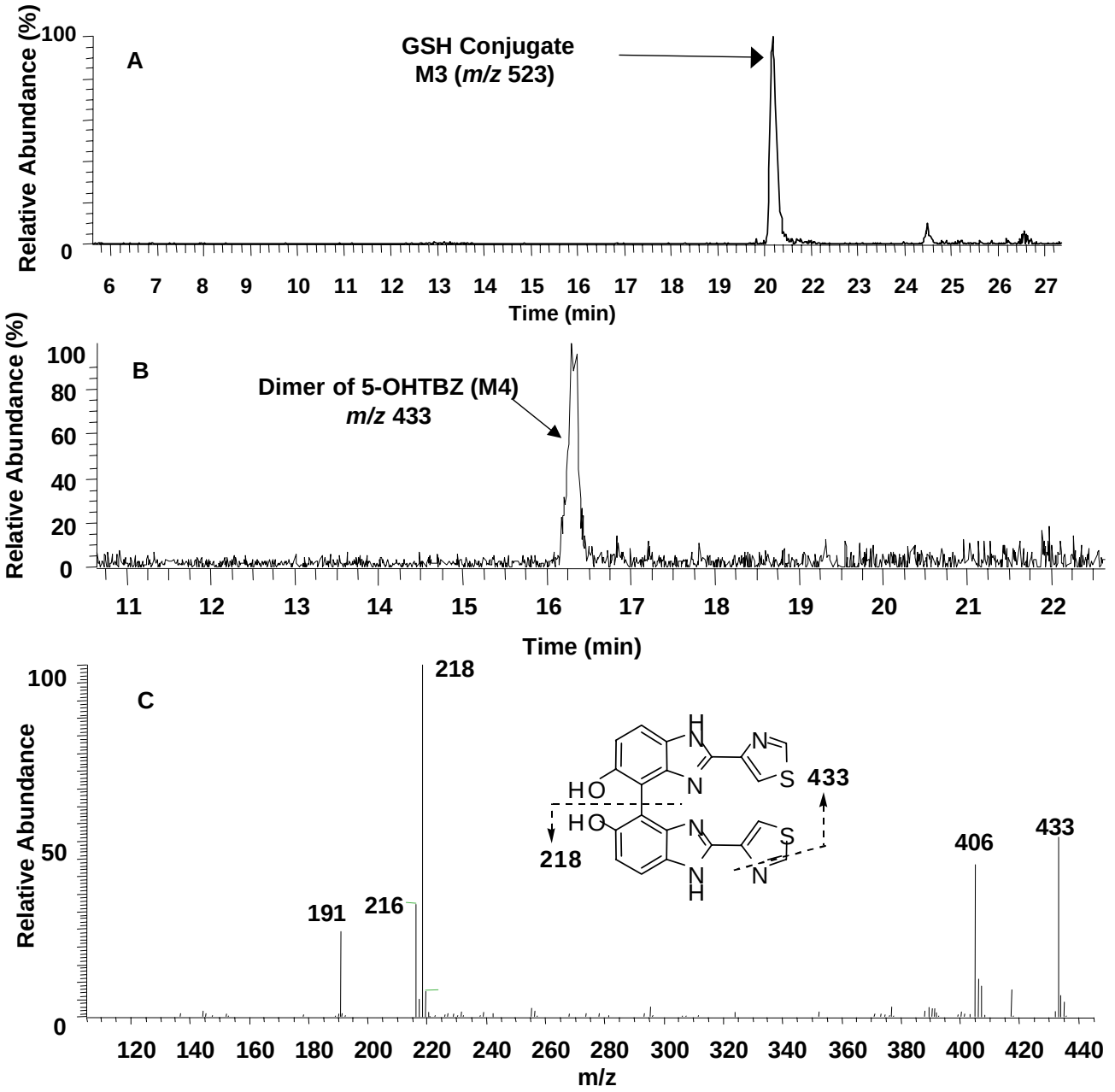

Figure 6

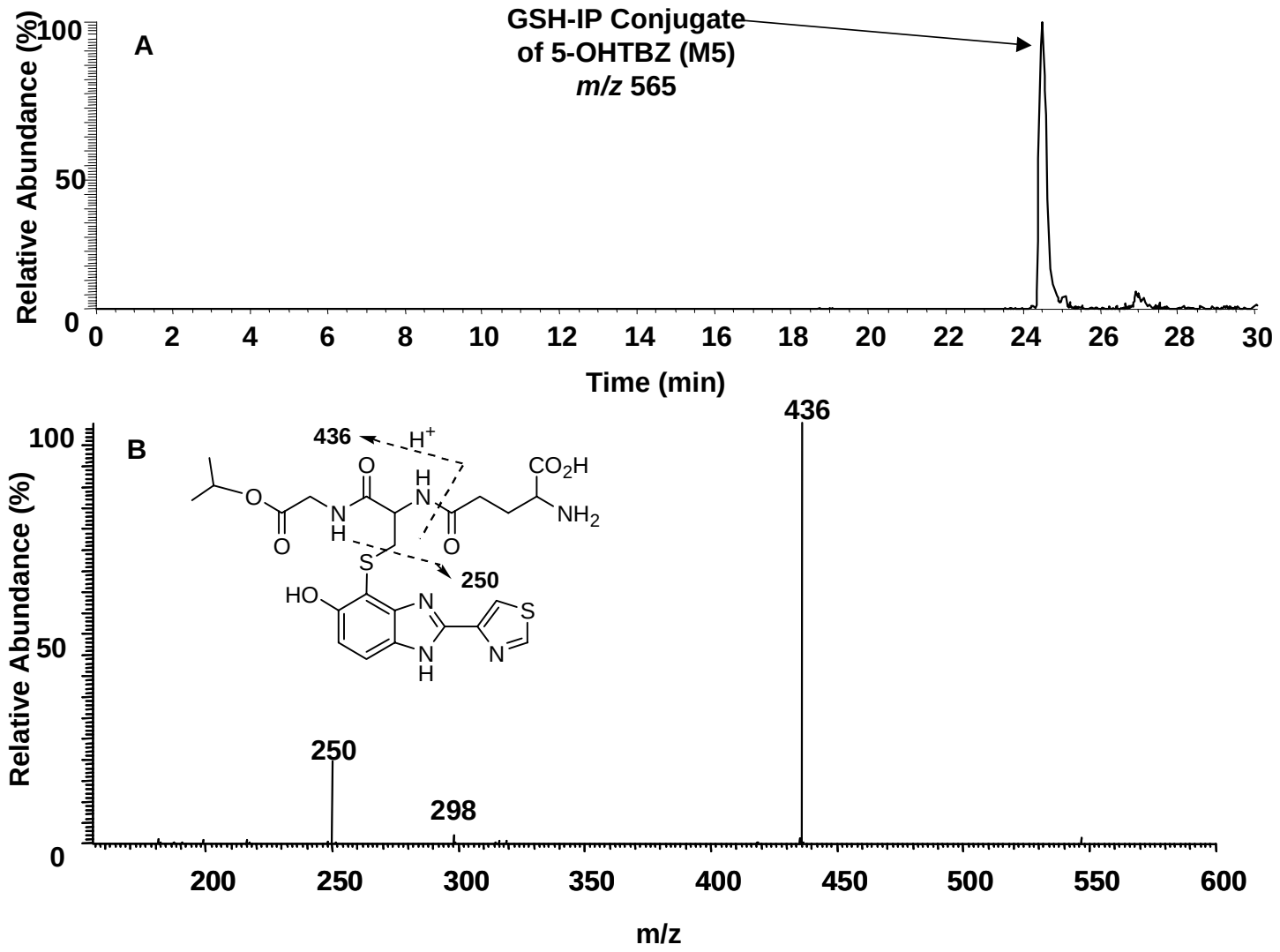

Figure 7

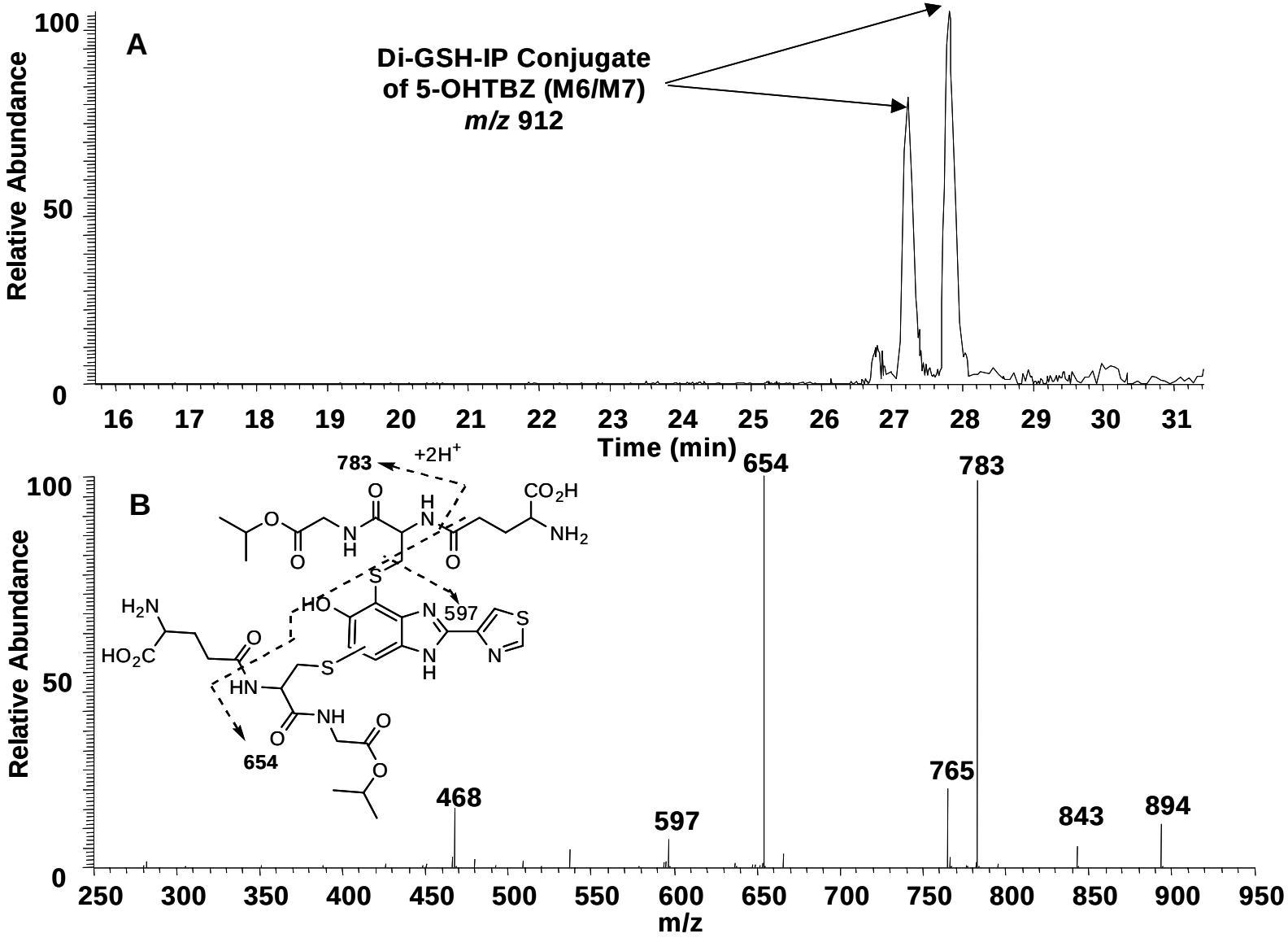

Figure 8

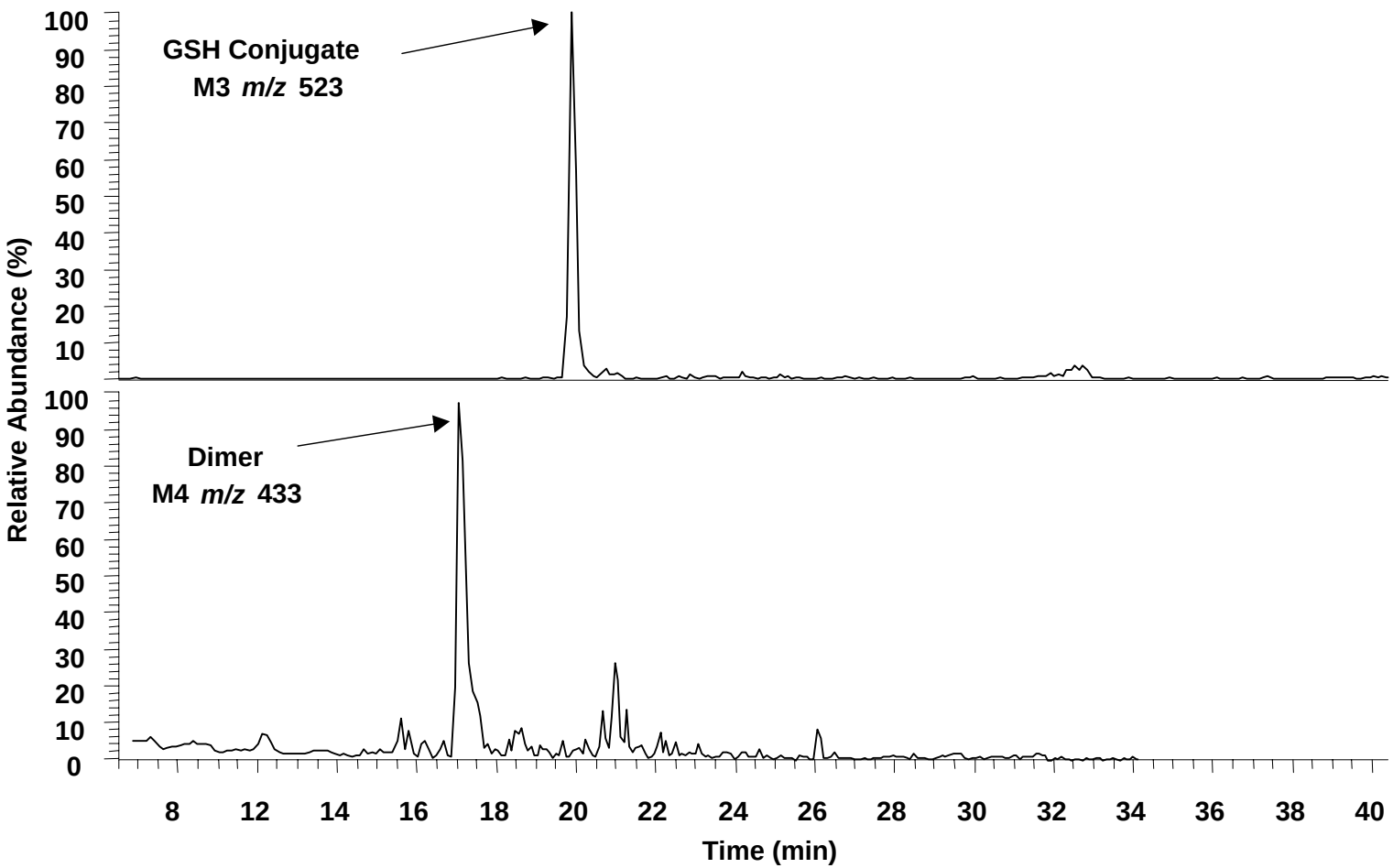

Scheme 1

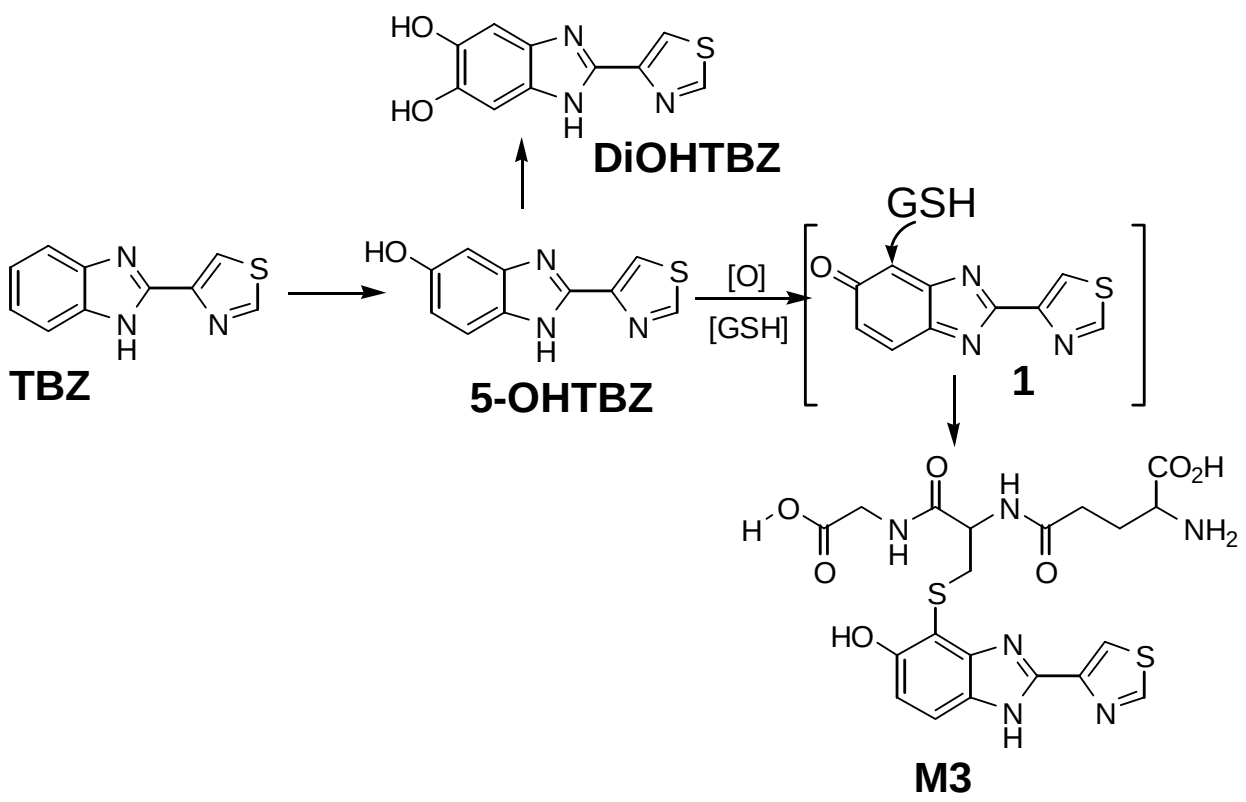

Scheme 2